Geological Magazine

www.cambridge.org/geo

$^{40}Ar/^{39}Ar$ age constraints for an early Alpine metamorphism of the Sakar unit, Sakar–Strandzha zone, Bulgaria

Nikolay Bonev[1], Richard Spikings[2] and Robert Moritz[2]

[1]Department of Geology, Paleontology and Fossil Fuels, Sofia University "St Kliment Ohridski", 1504 Sofia, Bulgaria and [2]Department of Earth Sciences, University of Geneva, CH-1205 Geneva, Switzerland

Rapid Communication

Cite this article: Bonev N, Spikings R, and Moritz R (2020) $^{40}Ar/^{39}Ar$ age constraints for an early Alpine metamorphism of the Sakar unit, Sakar–Strandzha zone, Bulgaria. *Geological Magazine* **157**: 2106–2112. https://doi.org/10.1017/S0016756820000953

Received: 27 May 2020
Revised: 14 July 2020
Accepted: 31 July 2020
First published online: 14 September 2020

Keywords:
$^{40}Ar/^{39}Ar$ geochronology; Sakar–Strandzha zone; Bulgaria

Author for correspondence:
Nikolay Bonev, E-mail: niki@gea.uni-sofia.bg

Abstract

We investigated the Sakar unit metamorphic rocks of the Sakar–Strandzha zone in Bulgaria, using $^{40}Ar/^{39}Ar$ dating of amphibole from the polymetamorphic basement and white mica in the overlying upper Permian metasedimentary rocks of the Paleokastro Formation. The amphibole and white mica revealed plateau ages of 140.50 ± 1.75 Ma and 126.19 ± 1.29 Ma, respectively, indicating an Early Cretaceous cooling history of the regional amphibolite-facies metamorphism to greenschist-facies conditions. Similar metamorphic grades and cooling histories of the Sakar unit share evidence with the nearby Rhodope Massif for the northern Aegean region-wide early Alpine tectonometamorphic event.

1. Introduction

The Sakar–Strandzha zone (Bonchev, 1903; Janichevski, 1946; Pamir & Baykal, 1947; Dimitrov, 1958; Aydin, 1974; Gocev, 1979, 1991; Dabovski & Zagorchev, 2009) is a major tectonic zone of the Alpine orogen in the northern Aegean region of the Eastern Mediterranean on the territories of Bulgaria and Turkey (Fig. 1, inset). It has been involved in pre-Alpine and Alpine tectonometamorphic events that have affected a Neoproterozic and mostly Palaeozoic high-grade metamorphic basement and its Triassic–Jurassic low-grade metasedimentary cover (Chatalov, 1988, 1990; Okay *et al.* 2001; Sunal *et al.* 2011; Bedi *et al.* 2013; Natal'in *et al.* 2016) (Fig. 1). Stratigraphic and tectonic relationships within the Sakar–Strandzha zone nappe pile, that is, the N-wards thrusting of the Triassic metasedimentary rocks onto both the Middle Jurassic (Bathonian) metasedimentary rocks and unmetamorphosed Upper Cretaceous (Cenomanian) sedimentary rocks (Chatalov, 1988, 1990), provided evidence for the Alpine tectonic and metamorphic history of the zone. U–Pb zircon dating of igneous and/or meta-igneous bodies and host metamorphic rocks in the Sakar–Strandzha zone revealed protracted Palaeozoic magmatic crystallization (Okay *et al.* 2001; Sunal *et al.* 2006; Natal'in *et al.* 2012; Georgiev *et al.* 2012; Machev *et al.* 2015; Bonev *et al.* 2019*a*), and also provided some information about early and late Palaeozoic metamorphic history (Okay *et al.* 2001; Natal'in *et al.* 2016; Bonev *et al.* 2019*a*), which was overprinted by Alpine metamorphism. The latter, which occured during Bathonian–Cenomanian time according to the stratigraphy, is also indicated by the same temporal spread of the available dates of mid- to low-temperature radioisotopic systems (Fig. 1).

Late Palaeozoic metamorphism in the Sakar–Strandzha zone was initially demonstrated by a whole-rock Rb–Sr age of 244 ± 11 Ma for the Kirklareli metagranite (see Fig. 1) (Aydin, 1974) at the Palaeozoic–Mesozoic boundary. U–Pb zircon dating in both the metagranites and the host high-grade basement gneisses, together with overlaping late Carboniferous – early Permian ages and common metamorphic fabric, was used as an argument for early Permian upper greenschist to lower amphibolite-facies metamorphism at *c.* 271 Ma linked to the Variscan orogeny (Okay *et al.* 2001). Lower amphibolite-facies metamorphism at the Carboniferous–Permian boundary was shown as the most obvious from the textures, field and U–Pb zircon geochronologic data for the Sakar–Strandzha zone metagranites and the host basement gneisses (Sunal *et al.* 2011; Machev *et al.* 2015; Bonev *et al.* 2019*a*). A pre-Middle Ordovician metamorphic event (*c.* < 484–450 Ma) was also inferred from the crystallization age of a magmatic body (Bonev *et al.* 2019*a*) and the detrital zircons contained in the high-grade basement and cover metasedimentary rocks (Sunal *et al.* 2008; Bonev *et al.* 2019*b*), which might extend to the Neoproterozoic–Cambrian (Natal'in *et al.* 2016).

Alpine metamorphism, which reaches greenschist facies in the metagranitoids (i.e. the Kirklareli metagranite), was revealed by a dark mica and whole-rock Rb–Sr isochron date of 155 ± 2 Ma, which was connected to N-directed thrusting related to middle Mesozoic orogeny (Okay *et al.* 2001). Upper greenschist- to epidote-amphibolite-facies metamorphism at a temperature (*T*) of 485–530°C and pressure (*P*) of 6–8 kbar is documented in the metagranitoids and the host basement gneisses, amphibolites and schists, and yields Rb–Sr muscovite and

CAMBRIDGE UNIVERSITY PRESS

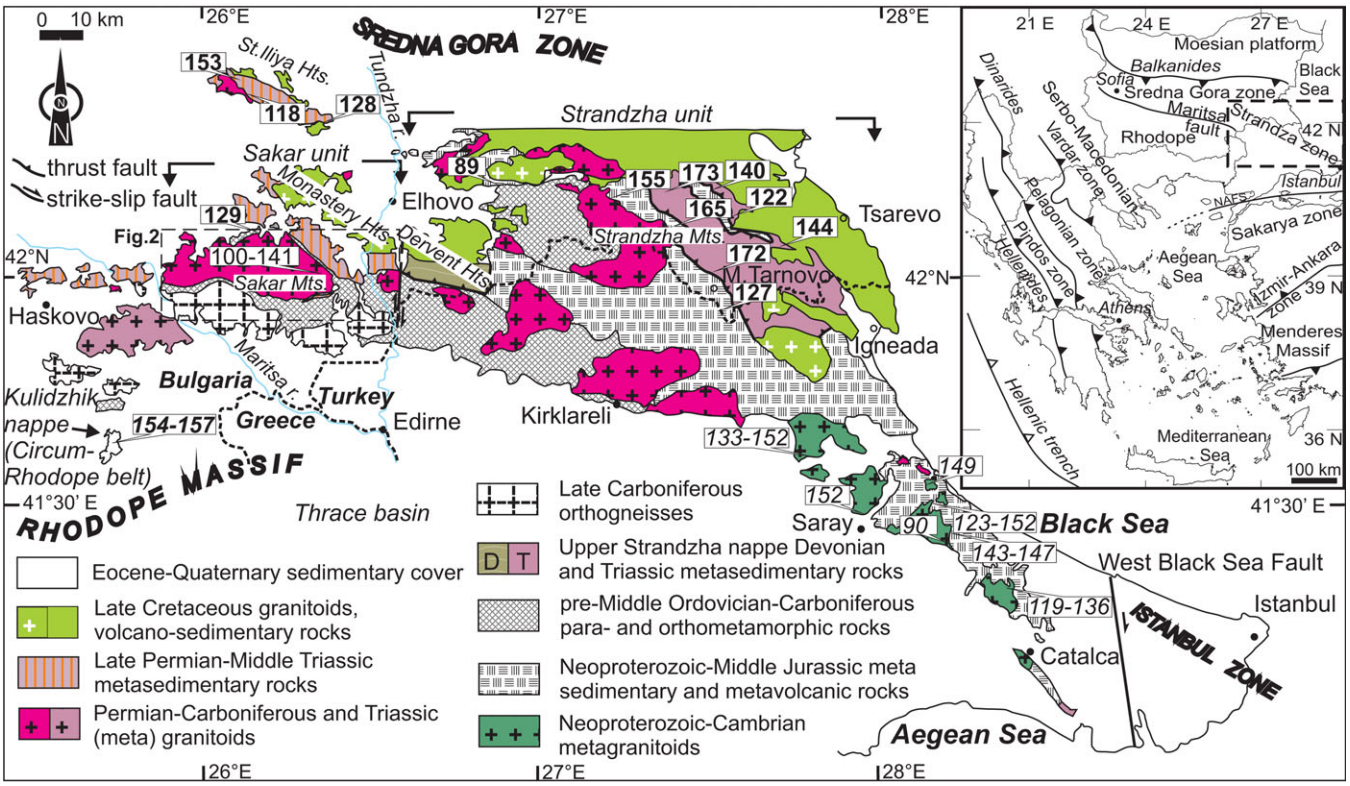

Fig. 1. (Colour online) Synthetic geological map of the Sakar–Strandzha zone in Bulgaria and Turkey (modified after Bonev *et al.* 2019*a*, *b*). Inset: Tectonic framework of the Alpine orogenic system in the northern Aegean region of the eastern Mediterranean domain. Geochronology: normal-font numbers: K–Ar ages (Boyadzhiev & Lilov, 1972; Palshin *et al.* 1989); bold: K–Ar ages (Lilov *et al.* 2004); italics: $^{40}Ar/^{39}Ar$ ages (Elmas *et al.* 2010); bold and italics: $^{40}Ar/^{39}Ar$ ages (Bonev *et al.* 2010).

biotite dates spanning 163–134 Ma (Sunal *et al.* 2011). The latter authors have interpreted these early Alpine metamorphic dates in a compressional, N-verging nappe tectonic context.

K–Ar ages of illite-muscovite in very-low-grade Jurassic phyllites and low-grade Triassic and Palaeozoic phyllites ($T = 350–450$°C; $P = 3–5$ kbar) in the Bulgarian part of the Sakar–Strandzha zone range from 118 Ma to 173 Ma, with an age of 123 Ma for the high-grade basement gneiss (Lilov *et al.* 2004). A dark mica K–Ar age of 133 Ma was also reported by Firsov (1975) for the high-grade basement schist. Lilov *et al.* (2004) have interpreted the K–Ar ages as recording Jurassic (160–170 Ma) (i.e. early Alpine) regional greenschist-facies metamorphism and subsequent resetting of the K–Ar system, yielding ages between 89 Ma and 128 Ma. Granitoids (i.e. Permian Sakar batholith) that intrude the high-grade metamorphic basement yield K–Ar dark mica ages that range from 100 Ma to 141 Ma (Boyadzhiev & Lilov, 1972; Palshin *et al.* 1989) (Fig. 1).

$^{40}Ar/^{39}Ar$ white and dark mica ages in the eastern Turkish part of the Sakar–Strandzha zone encompass 119–152 Ma interval in the metagranitoids, 123–138 Ma in the high-grade basement and 143–152 Ma in the Triassic–Jurassic metasedimentary rocks (Elmas *et al.* 2010) (see Fig. 1), interpreted to date cooling of the Alpine metamorphism and exhumation of the metamorphic pile in an extensional tectonic context. Neubauer *et al.* (2010) report $^{40}Ar/^{39}Ar$ ages of amphibole and white mica ranging over 136–144 Ma in the Sakar unit of the Sakar–Strandzha zone (see Fig. 1), which they interpret to date ductile, mylonitic deformation along the contact of the Sakar batholith and the host high-grade basement metamorphic rocks. According to Neubauer *et al.* (2010), the white mica age decreased to *c.* 124 Ma further south in the basement metamorphic rocks, due to an initial thermal overprint and a subsequent overprint at *c.* 69 Ma. Recently, hydrothermal activity in the Sakar batholith was bracketed between 149 ± 7 Ma and 114 ± 1 Ma by U–Pb apatite and titanite dates, respectively (Szopa *et al.* 2020), which questions temporal relationships between Alpine metamorphism and hydrothermal activity. Finally, early Alpine metamorphism in the Sakar–Strandzha zone was succeeded by erosion-driven, slow-cooling-exhumation during Late Cretaceous – Eocene time, as derived from the apatite fission-track data (Cattò *et al.* 2017).

More precise age constraints for the protracted Alpine metamorphism (89–173 Ma) of the Sakar–Strandzha zone are critical to improve our understanding of the timing of its tectonometamorphic history, which also requires an assessment of the regional-scale links. Here, we apply $^{40}Ar/^{39}Ar$ dating of metamorphic rocks in the Sakar unit of the Sakar–Strandzha zone in Bulgaria (Figs 1, 2), with the aim of constraining more precisely the timing of early Alpine metamorphism, which is highly relevant to the Mesozoic evolution of the Alpine orogen in the northern Aegean region.

2. Geological outline of the Sakar unit

The pre-Upper Cretaceous geology of the Sakar unit is dominated by felsic igneous and meta-igneous bodies and high-grade country metamorphic basement rocks, which are overlain by Triassic metasedimentary rocks. They are subdivided into five subunits that include (Fig. 2): (i) a variegated complex of the high-grade basement equated to the Rhodope Massif high-grade basement (Kozhoukharov, 1987); (ii) the Lesovo gneiss-granite complex (Boyanov *et al.* 1965) and the intruded leucocratic dyke and stock granitoid bodies; (iii) the Melnitsa orthometamorphic complex

https://doi.org/10.1017/S0016756820000953 Published online by Cambridge University Press

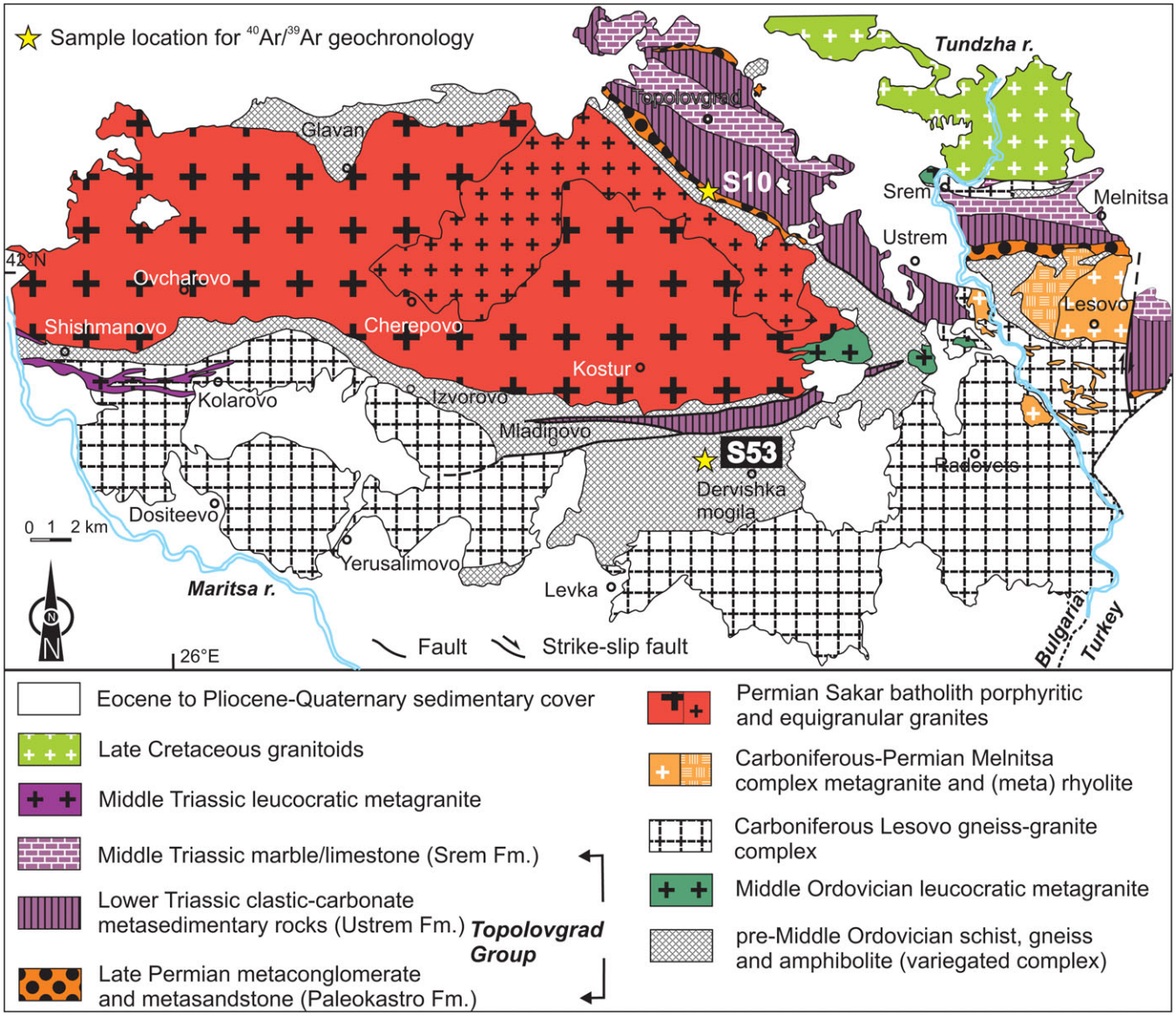

Fig. 2. (Colour online) Geological map of the Sakar unit (compiled after Kozhoukharova & Kozhoukharov, 1973; Savov & Dabovski, 1980; Chatalov, 1992; Dabovski *et al.* 1994) showing the locations of the samples studied for $^{40}Ar/^{39}Ar$ geochronology. Age results for the geologic subunits are incorporated in the map after Bonev *et al.* (2019*a*, *b*, *c*).

(Chatalov, 1992); (iv) the Sakar granitoid batholith (Boyanov *et al.* 1965; Dabovski & Haydoutov 1980; Kamenov *et al.* 2010); and (v) the Sakar-type metasedimentary rocks of the Lower–Middle Triassic Topolovgrad Group (Chatalov, 1990, 1991). The Upper Cretaceous – Quaternary subunits are beyond the scope of the paper.

The variegated complex consists of intercalated schist, gneiss and amphibolite of inferred Precambrian age (e.g. Kozhoukharov, 1987). Similar high-grade basement lithologies in Turkey yielded Proterozoic–Permian (2450–271 Ma) detrital zircon dates (Sunal *et al.* 2008; Natal'in *et al.* 2012). Fossil evidence indicates uppermost Ordovician – middle Silurian (Lakova *et al.* 1992), Lower Devonian (Zacharieva-Kovacheva *et al.* 1964; Malyakov & Prokop, 1997) and lower Permian (Malyakov & Bakalova, 1978) protoliths of the crystalline basement schist in the Sakar–Strandzha nappe stack. Tschermakite-bearing amphibolites in the variegated complex have island-arc basalt protoliths and record metamorphic conditions of $T = 625–635$°C and $P = 6.5–8$ kbar (Chavdarova & Machev, 2017). The same amphibole composition as the amphibolites of the same subunit in Turkey is considered to have recrystallized during the latest metamorphic event of Alpine age (Sunal *et al.* 2011).

The Lesovo gneiss-granite complex consists mostly of texturally distinct gneiss of granodioritic-dioritic composition (Boyanov *et al.* 1965; Kozhoukharova & Kozhoukharov, 1973), which has a latest Carboniferous protolith age of 305.8 ± 1.4 Ma (Bonev *et al.* 2019*a*). E–W-oriented leucocratic dykes and stock-like bodies cross-cut the variegated complex and the Lesovo complex. A stock-like body crystallized at the eastern margin of the Sakar batholith during Middle Ordovician time (461.6 ± 2.7 Ma), whereas a leucocratic dyke exposed at the western margin of the batholith has a Middle Triassic crystallization age (242.1 ± 1.8 Ma, Bonev *et al.* 2019*b*).

The Melnitsa orthometamorphic complex (e.g. Chatalov, 1992) is a volcano-plutonic complex that consists of calc-alkaline porphyritic metagranite, (meta)granite-porphyries and (meta)rhyolite located east of the Sakar batholith and within the Lesovo complex (Fig. 2). The porphyritic metagranite and the (meta)rhyolite of

https://doi.org/10.1017/S0016756820000953 Published online by Cambridge University Press

the Melnitsa complex crystallized at 300.2 ± 3.4 Ma and 297.2 ± 4.6 Ma, respectively (Bonev *et al.* 2019*a*).

The undeformed and unmetamorphosed Sakar granitoid batholith is an E–W-aligned elongated dome-like body (Fig. 2). It mainly consists of calc-alkaline K-feldspar porphyritic granite and equigranular granite types (Dabovski & Haydoutov, 1980; Kamenov *et al.* 2010), which crystallized at 296.1 ± 2.7 Ma and 295.3 ± 1.9 Ma, respectively (Bonev *et al.* 2019*a*).

As the Sakar batholith contains well-foliated and folded gneiss, schist and amphibolite xenoliths from the variegated complex, this feature indicates a pre-Permian high-grade metamorphism and deformation. Both processes are also confirmed by the Lesovo complex that contains gneiss and schist xenoliths. The Melnitsa complex is less deformed and less metamorphosed compared with all other mentioned metamorphic basement subunits.

The Topolovgrad Group unconformably overlies the variegated complex and consists of Triassic metasedimentary rocks that have been subdivided into three formations in the following stratigraphic order (Chatalov, 1990, 1991). The lower clastic Paleokastro Formation passes into the clastic-carbonate Ustrem Formation, whose upper levels contain latest Early Triassic bivalves, which is in turn overlain by the Middle Triassic, conodont-bearing carbonate Srem Formation. The Sakar batholith and the Melnitsa complex magmatic rocks have been reworked as pebbles and clasts in the sedimentary fill of the Paleokastro Formation (Boyanov *et al.* 1965; Dabovski & Haydoutov, 1980; Chatalov, 1990, 1991, 1992). U–Pb detrital zircon geochronology from the base of the Paleokastro Formation up to the middle stratigraphic levels of the Ustrem Formation revealed a late Permian maximum depositional age of 259.1 ± 5.8 Ma (Bonev *et al.* 2019*c*). The Topolovgrad Group is interpreted as a fluvial–alluvial succession, starting with the basal Paleokastro Formation that progressively fines upwards into the Ustrem Formation, passing upwards into a shallow-water carbonate platform of the Srem Formation, all of which were deposited in a Triassic sedimentary basin (Chatalov, 1991). A superimposed metamorphic conformity was proposed for the position of the Paleokastro Formation onto the variegated complex (Savov & Dabovski, 1980) and onto the Melnitsa complex (Chatalov, 1992). The metamorphic grade of the Topolovgrad Group reaches a low-temperature amphibolite facies, with muscovite–biotite–almandine garnet ± staurolite ± kyanite, which defines metamorphic conditions of $T = 520–550$°C and $P = 2.5–9$ kbar for the metapelitic rocks of the Ustrem Formation (Chatalov, 1990). Chavdarova & Machev (2017) have reported metamorphic conditions of $T = 510–555$°C and $P = 6–8$ kbar in the amphibolites of the Ustrem Formation. Quartz–biotite–muscovite schist intercalations are present in metaconglomerate and arkosic metasandstone, which are the most common rock types of the Paleokastro Formation. The Ustrem Formation has an irregular alternation of the main rock types of quartz–mica schist with biotite and garnet ± staurolite porphyroblasts, marbles, quartz–mica–calcite schist with biotite porphyroblasts, and subordinate metasandstone and amphibolite. The Srem Formation consists of calcite and dolomite marbles. The metamorphism associated with a weak deformation progressively decreases up the stratigraphic section of the Topolovgrad Group. The metamorphism of the Topolovgrad Group is related to the N-verging nappe-staking event either at the end of the Triassic Period (i.e. based on the age of the Srem Formation) or during post-Middle Jurassic time (i.e. based on the youngest Jurassic rocks in the Sakar–Strandzha zone).

3. Samples and $^{40}Ar/^{39}Ar$ results

We focused on key lithologies in the subunits of the Sakar unit, which include an amphibolite from the variegated complex of the high-grade basement and a metasandstone from the Paleokastro Formation of the Topolovgrad Group. Sample numbers mentioned below refer to sample locations depicted in Figure 2, which are given with their coordinates in online Supplementary Table S1 (available at http://journals.cambridge.org/geo).

Field observations of the high-grade basement south of the Sakar batholith revealed a kilometre-thick and regional foliation-parallel amphibolite sequence within the variegated complex, located to the west of the village of Dervishka mogila (Fig. 2). This amphibolite sequence might represent an original mafic sill-like body emplaced in a sedimentary succession, and then both metamorphosed to amphibolite facies. The fine- to medium-grained amphibolite (sample S53) mainly consists of amphibole, quartz and plagioclase (Fig. 3a). Subordinate metamorphic mineral phases are epidote, ilmenite and biotite. Prismatic to elongated needle-like green amphibole is inter-grown with the later mineral phases. Accessories include zircon and apatite. The amphibole defines the foliation both macro- and microscopically, and the quartz is slightly recrystallized.

Metasandstone sample S10 of the Paleokastro Formation was sampled from its uppermost stratigraphic level just below the first quartz–chlorite–muscovite schist with biotite porphyroblasts of the Ustrem Formation (Fig. 2). The coarse-grained metasandstone contains rare quartz clasts that locally delineate thin discontinuous layers of matrix-supported metaconglomerate. Metasandstone S10 is a two-mica schist consisting of quartz, alkali feldspar, and dark and white mica in modally decreasing abundances. Quartz is moderately sorted, showing large mono- and polycrystalline grains, the smaller of which are recrystallized. Alkali feldspar has the same sorting and is perthitic microcline. Brown-green dark mica forms large flakes of different orientation relative to the foliation. White mica mostly defines a discontinuous foliation that anastomoses the clastic grains. Micas overgrew these grains or grew in their interstices. Magnetite grains and aggregates and rare quartz–feldspar lithic fragments also occur. Accessory minerals include apatite, zircon and rutile.

Amphibole in amphibolite S53 and white mica in metasandstone S10 were separated for $^{40}Ar/^{39}Ar$ dating from a 250–400-μm sieve fraction using conventional magnetic and heavy liquid methods. The mineral concentrates were purified by hand-picking under a binocular microscope. $^{40}Ar/^{39}Ar$ analyses were conducted at the University of Geneva using an Argus VI (Thermo Fischer Scientific) multi-collector mass spectrometer. ^{40}Ar was collected using a Faraday collector with a feedback resistance of 1×10^{12} Ohms, whereas $^{39–36}Ar$ was collected on a Faraday collector with a feedback resistance of 1×10^{13} Ohms. Analytical details and procedures are as described in Villagómez & Spikings (2013). All dates were calculated from blank- and baseline-corrected measurements, while mass discrimination was monitored by analyses of air aliquots after every 10 heating steps (online Supplementary Table S1). Neutron irradiation was monitored using Fish Canyon Tuff Sanidine, with a $^{40}Ar/^{39}Ar$ age of 28.201 ± 0.046 Ma (Kuiper *et al.* 2008). Gas was liberated from the samples using an infrared laser (Photon Machines Inc.), and cleaned in an ultra-high vacuum steel extraction line equipped with a cold finger at −132°C and a GP50 (ST101) getter. The $^{40}Ar/^{39}Ar$ age spectra and $^{36}Ar/^{40}Ar$ to $^{39}Ar/^{40}Ar$ isochron ages are shown in Figure 4, all with a corresponding 2σ analytical error.

https://doi.org/10.1017/S0016756820000953 Published online by Cambridge University Press

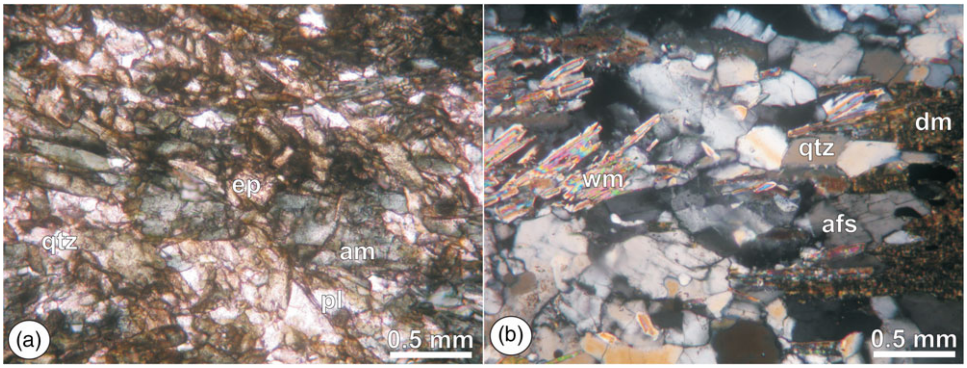

Fig. 3. (Colour online) Microphotographs of the samples used for $^{40}Ar/^{39}Ar$ geochronology in the Sakar unit. (a) Amphibolite (sample S53) from the variegated complex of the high-grade metamorphic basement showing recrystallization under amphibolite-facies conditions, plane-polarized light. (b) Two-mica schist (sample S10) from the Paleokastro Formation, cross-polarized light. am – amphibole; dm – dark mica; ep – epidote; afs – alkali feldspar; qtz – quartz; wm – white mica; pl – plagioclase.

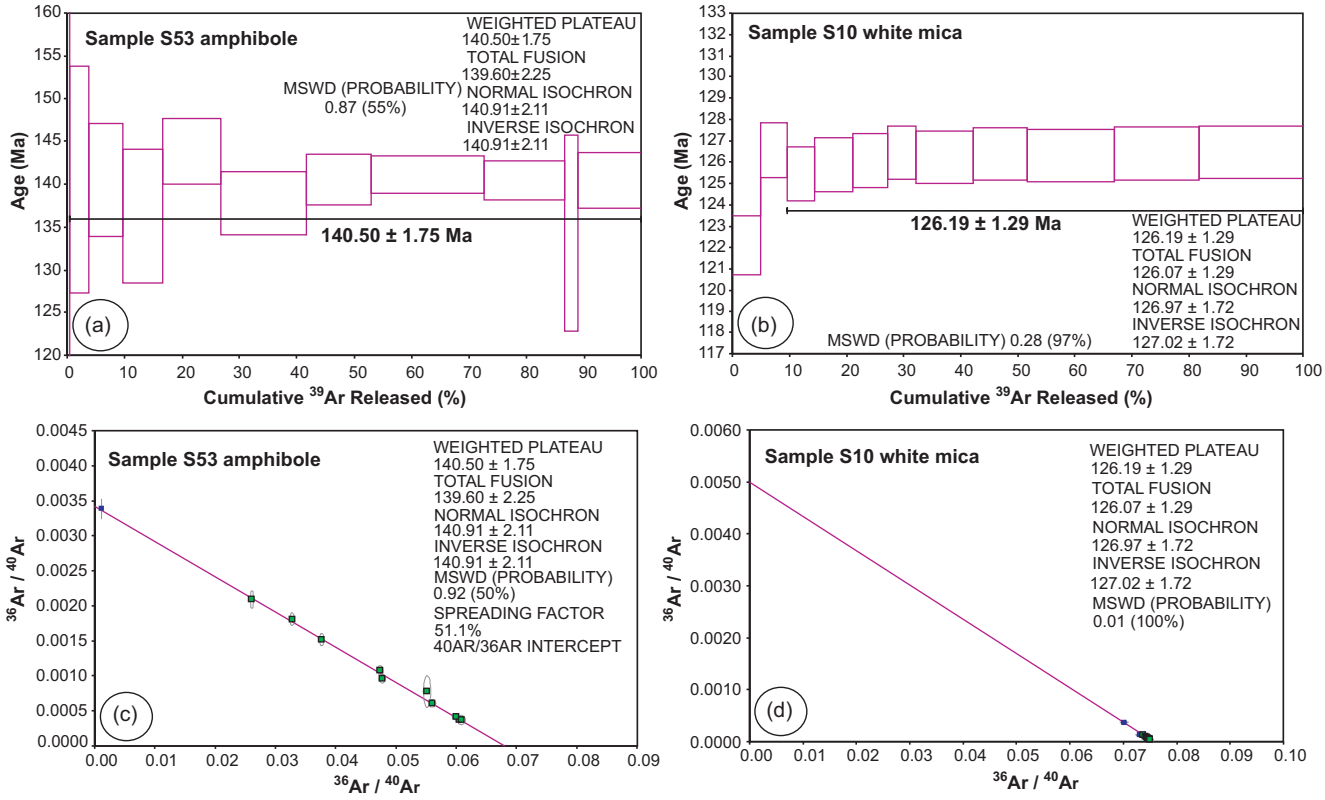

Fig. 4. (Colour online) $^{40}Ar/^{39}Ar$ geochronology results for the samples S53 and S10 from the Sakar unit. (a, b) $^{40}Ar/^{39}Ar$ age spectra and (c, d) $^{36}Ar/^{40}Ar$ to $^{39}Ar/^{40}Ar$ isochron ages. For the sample locations see Figure 2.

Amphibole from amphibolite S53 yields a $^{40}Ar/^{39}Ar$ plateau date of 140.50 ± 1.75 Ma from 100% of the ^{39}Ar released (in 10 steps; Fig. 4a), which overlaps with the inverse isochron date of 140.91 ± 2.11 Ma (Fig. 4c). White mica from metasandstone S10 gave a plateau $^{40}Ar/^{39}Ar$ date of 126.19 ± 1.29 Ma from nine steps (90% of the total ^{39}Ar released), which overlaps with the inverse isochron age of 127.02 ± 1.72 Ma (Fig. 4b, d).

4. Discussion

The mineral assemblages and textures in the dated samples show that the white mica and amphibole recrystallized during amphibolite-facies metamorphism, at temperatures above their closure temperatures range for argon in white mica (*c.* 440°C, Harrison *et al.* 2009) and in amphibole (535 ± 50°C) (e.g. Harrison, 1981; McDougall & Harrison, 1999). The new $^{40}Ar/^{39}Ar$ ages therefore determine the cooling histories of the dated metamorphic rocks within 535–440°C, after the peak of the regional amphibolite-facies metamorphism. This temperature window coincides with greenschist-facies metamorphism within the crust, and therefore constrains the timing of the transition to such conditions of the metamorphic pile.

The $^{40}Ar/^{39}Ar$ date of 140.50 ± 1.75 Ma of amphibolite S53 from the variegated complex, which constitutes the country rocks of the Sakar batholith, indicates that the high-grade metamorphic basement cooled below *c.* 500°C during earliest Cretaceous time. The amphibole defines the planar metamorphic fabric in the rock (Fig. 3a) and shows that the cooling age that developed during Ar closure in this mineral testifies to the end of regional amphibolite-facies metamorphism. The white mica date of metasandstone S10

https://doi.org/10.1017/S0016756820000953 Published online by Cambridge University Press

indicates that the Paleokastro Formation cooled below *c.* 440–400°C at 126.19 ± 1.29 Ma, subsequent to amphibolite-facies metamorphism, when the temperatures regressed to greenschist-facies conditions. This interpretation fits the regional time scale provided by the K–Ar and $^{40}Ar/^{39}Ar$ mica dates for the cooling stage towards greenschist-facies conditions in the Sakar–Strandzha zone of 173–100 Ma (see Fig. 1), subsequent to epidote-amphibolite-facies metamorphism at 163–134 Ma (Sunal *et al.* 2011) or *c.* 155 Ma (Okay *et al.* 2001) as derived from the Rb–Sr ages.

$^{40}Ar/^{39}Ar$ geochronologic results for the Sakar unit should be considered within a broad regional context, including the adjacent Rhodope Massif, located just to the south of this unit (Fig. 1). This is based on the recent geochronologic record of Middle Triassic magmatism on both sides of the Maritsa river valley, which demonstrates the extension of the Sakar unit up to the limit of the eastern Rhodope Massif (Bonev *et al.* 2019*b*; see Fig. 1).

There are field, textural and U–Pb zircon geochronologic evidence for Late Jurassic amphibolite-facies metamorphism at 160–154 Ma (Bonev *et al.* 2015), or high-pressure metamorphism at 158–150 Ma (Liati *et al.* 2011, 2016) in the eastern Rhodope Massif. The amphibolite-facies metamorphism is temporarily connected with the upper greenschist-facies metamorphism at 157–154 Ma, which is coeval with the emplacement of the Kulidzhik nappe from the Circum–Rhodope belt on top of the Rhodope metamorphic pile, as determined using $^{40}Ar/^{39}Ar$ geochronology (Bonev *et al.* 2010). The overlap of the K–Ar and $^{40}Ar/^{39}Ar$ ages of the Sakar–Strandzha zone and the $^{40}Ar/^{39}Ar$ ages of the Circum–Rhodope belt in the eastern Rhodope Massif (see Fig. 1) indicate that cooling of amphibolite-facies metamorphism and the thermal transition to upper greenschist metamorphism was a common event for both areas. A similar early Mesozoic stratigraphy of the Sakar–Strandzha zone and the Circum–Rhodope belt in the eastern Rhodope Massif was emphasized due to their tight facial and temporal relationships in a single zone linked to common N-wards nappe emplacement (Gocev, 1979, 1991; Chatalov 1988, 1990). Subsequent studies in the Sakar–Strandzha zone and the Circum–Rhodope belt have confirmed the metamorphic grade and temporal spread of Late Jurassic – Early Cretaceous thrust tectonics (Okay *et al.* 2001; Bonev & Stampfli, 2011; Sunal *et al.* 2011; Bonev *et al.* 2015; Natal'in *et al.* 2016). The new $^{40}Ar/^{39}Ar$ ages obtained for the Sakar unit further confirm regional-scale correlations between the eastern Rhodope Massif and the Sakar–Strandzha zone with respect to the early Alpine tectonic and metamorphic evolution, providing evidence for Early Cretaceous cooling after amphibolite-facies metamorphism.

5. Conclusions

Our $^{40}Ar/^{39}Ar$ isotopic study shows that early Alpine regional amphibolite-facies metamorphism of the Sakar unit cooled through *c.* 550–440°C during Early Cretaceous time (*c.* 141–126 Ma) towards greenschist-facies conditions. Time constraints for cooling retrogression from the amphibolite-facies metamorphism, which initiated during Late Jurassic time in the Sakar–Strandzha zone, reveal an equivalent temporal metamorphic history with amphibolite- to greenschist-facies metamorphism of the Circum–Rhodope belt, and common Late Jurassic – Early Cretaceous regional-scale thrust tectonics.

Supplementary material. To view supplementary material for this article, please visit https://doi.org/10.1017/S0016756820000953

Acknowledgements. The study was supported by the Bulgarian National Science Fund project no. DN 04/6. We thank both anonymous reviewers for their comments, as well as the editorial comments, which helped us to improve the paper.

References

Aydin Y (1974) Etude pétrographique et géochemique de la partie centrale du Massif d'Istranca (Turque). PhD thesis, University of Nancy, France. Published thesis.

Bedi Y, Vasilev E, Dabovski Ch, Ergen A, Okuyucu C, Do an A, Tekin UK, Ivanova D, Boncheva I, Lakova I, Sachanski V, Kuşcu I, Tuncay E, Demiray DG, Soycan H and Göncüoglu MC (2013) New age data from the tectonistratigraphic units of the Istranca "Massif" in NW Turkey: a correlation with SE Bulgaria. *Geologica Carpathica* **64**, 255–77.

Bonchev G (1903) Petrographic description of the southeastern part of Bulgaria. *Periodic Journal of the Bulgarian Booklet Society* **54**, 1–95.

Bonev N, Filipov P, Raicheva R and Moritz R (2019a) Timing and tectonic significance of Paleozoic magmatism in the Sakar unit of the Sakar-Strandzha zone, SE Bulgaria. *International Geology Review* **61**, 1957–79.

Bonev N, Filipov P, Raicheva R and Moritz R (2019b) Triassic magmatism along the Maritsa river valley, Sakar-Strandzha zone, Bulgaria. *Review of the Bulgarian Geological Society* **80**, 56–7.

Bonev N, Filipov P, Raicheva R and Moritz R (2019c) Detrital zircon age constraints on the deposition of the Topolovgrad Group, Sakar-Strandzha Zone, SE Bulgaria. *Geophysical Research Abstracts* **21**, 1 pp. paper EGU 2019-1921-1.

Bonev N, Marchev P, Moritz R and Collings D (2015) Jurassic subduction zone tectonics of the Rhodope Massif in the Thrace region (NE Greece) as revealed by new U-Pb and $^{40}Ar/^{39}Ar$ geochronology of the Evros ophiolite and high-grade basement rocks. *Gondwana Research* **27**, 760–75.

Bonev N, Spikings R, Moritz R and Marchev P (2010) The effect of early Alpine thrusting in late-stage extensional tectonics: Evidence from the Kulidzhik nappe and the Pelevun extensional allochthon in the Rhodope Massif, Bulgaria. *Tectonophysics* **488**, 256–81.

Bonev N and Stampfli G (2011) Alpine tectonic evolution of a Jurassic subduction-accretionary complex: Deformation, kinematics and $^{40}Ar/^{39}Ar$ age constraints on the Mesozoic low-grade schists of the Circum-Rhodope Belt in the eastern Rhodope-Thrace region, Bulgaria-Greece. *Journal of Geodynamics* **52**, 143–67.

Boyadzhiev S and Lilov P (1972) On the age data for the southbulgarian granitoids from the Sredna Gora and Sakar-Strandzha zones determined by K-Ar method. *Bulletin of the Geological Institute –Geochemistry, Mineralogy and Petrography* **21**, 211–20.

Boyanov I, Kozhoukharov D and Savov S (1965) Geological structure of the southern slope of the Sakar Mountains between the villages of Radovets and Kostour. *Review of the Bulgarian Geological Society* **26**, 121–34.

Cattò S, Cavazza W, Zattin M and Okay AI (2017) No significant Alpine tectonic overprint on the Cimmerian Strandja Massif (SE Bulgaria and NW Turkey). *International Geology Review* **147**, 404–16.

Chatalov A (1992) Petrological characteristics of the rocks of Melnitsa orthometamorphic complex, Sakar Mountains. *Review of the Bulgarian Geological Society* **53**, 99–112.

Chatalov GA (1988) Recent developments in the geology of the Strandzha zone in Bulgaria. *Bulletin of the Technical University Istanbul* **41**, 433–65.

Chatalov GA (1990) *Geology of the Strandzha Zone in Bulgaria*. Publishing house of Bulgarian Academy of Sciences, Sofia, Geologica Balcanica, Operum Singulorum 4, pp. 263.

Chatalov G (1991) Triassic in Bulgaria – a review. *Bulletin of the Technical University Istanbul* **41**, 433–65.

Chavdarova S and Machev Ph (2017) Amphibolites from Sakar Mountain – geological position and petrological features. Proceedings of *Annual Conference of the Bulgarian Geological Society (Geosciences 2017)*, Sofia, 7–8 December 2017. Bulgarian Geological Society, Sofia, 49–50.

Dabovski Ch and Haydoutov I (1980) The Sakar pluton. In *The Precambrian in South Bulgaria* (eds Kozhoukharov D and Dabovski Ch), pp. 83–89. Bulgaria, October 1980, Bulgarian Academy of Sciences, Geological Institute, Guide to Excursion IGCP project 22.

Dabovski Ch, Savov S, Chatalov G and Shiliafov G (1994) Geological map of Bulgaria, scale 1:100 000: Map sheet Elhovo, Committee of Geology and Mineral Resources, Geology and Geophysics Corp.

Dabovski Ch and Zagorchev I (2009) Introduction: Mesozoic evolution and Alpine structure. In *Geology of Bulgaria*, Volume 2, Part 5, Mesozoic Geology (eds I Zagorchev, C Dabovski and T Nikolov), pp. 13–30. Sofia: Academic Publisher Prof. Marin Drinov.

Dimitrov S (1958) Über die alpidische Regionalmetamorphose und ihre Beziehungen zu der Tektonik und dem Magmatismus in Südostbulgarien. *Geologie* **7**, 560–8.

Elmas A, Yilmaz Y, Yigitbas N and Ulrich T (2010) A Late Jurassic-Early Cretaceous metamorphic core complex, Strandja Massif, NW Turkey. *International Journal of Earth Sciences* **100**, 1251–63.

Firsov L (1975) On the age of the South-Bulgarian granitoids of the Rhodope Massif, Srednogorie and Sakar-Strandzha. *Geology and Geophysics (Sofia)* **1**, 27–34.

Georgiev S, von Quadt A, Heinrich C, Peytcheva I and Marchev P (2012) Time evolution of rifted continental arc: integrated ID-TIMS and LA-ICPMS study of magmatic zircons from the Eastern Srednogorie, Bulgaria. *Lithos* **154**, 53–67.

Gocev P (1979) The place of Strandza in the Alpine structure of the Balkan Peninsula. *Review of the Bulgarian Geological Society* **30**, 27–46.

Gocev PM (1991) Some problems of the nappe tectonics of the Strandzides in Bulgaria and Turkey. *Bulletin of the Technical University Istanbul* **44**, 137–64.

Harrison TM (1981) Diffusion of ^{40}Ar in hornblende. *Contributions to Mineralogy and Petrology* **78**, 324–31.

Harrison TM, Célérier J, Aikman AB, Hermann J and Heizler MT (2009) Diffusion of ^{40}Ar in muscovite. *Geochimica and Cosmochimica Acta* **73**, 1039–51.

Janichevski A (1946) Aperçu abrège sur la géologie de la montagne Strandja dans la Bulgarie de sud-est. In *Géologie de la Bulgarie* (eds FR Cohen, Tz Dimitroff and B Kamenov), pp. 380–89. Department of Geology and Mining, Sofia, Annuaire de la direction pour les recherches géologiques et minières A4.

Kamenov BK, Vergilov V, Dabovski Ch, Vergilov I and Ivchinova L (2010) The Sakar batholith – petrology, geochemistry and magmatic evolution. *Geochemistry, Mineralogy and Petrology (Sofia)* **48**, 1–37.

Kozhoukharov D (1987) Lithostratigraphy and structure of Precambrian in the core of the Byala reka dome in the Eastern Rhodope. *Geologica Balcanica* **17**, 15–39.

Kozhoukharova E and Kozhoukharov D (1973) Stratigraphy and petrology of the Precambrian metamorphic rocks from the Sakar Mountain. *Bulletin of the Geological Institute –Geochemistry, Mineralogy and Petrography* **22**, 193–210.

Kuiper K, Deino A, Hilgen F, Krijgsman W, Renne P and Wijbrans JR (2008) Synchronizing rock clocks of Earth history. *Science* **320**, 500–4.

Lakova I, Gocev P and Yanev S (1992) Palynostratigraphy and geological setting of the Lower Paleozoic allochthon in Dervent Heights, SE Bulgaria. *Geologica Balcanica* **22**, 71–88.

Liati A, Gebauer D and Fanning CM (2011) Geochronology of the Alpine UHP Rhodope zone: A review of isotopic ages and constraints on the geodynamic evolution. In *Ultrahigh-Pressure Metamorphism 25 Years after the Discovery of Coesite and Diamond* (eds LF Dobrzhinetskaya, SW Faryad, S Wallis and S Cuthbert), pp. 295–324. Elsevier, Amsterdam.

Liati A, Theye T, Fanning CM, Gebauer D and Rainer N (2016) Multiple subduction cycles in the Alpine orogeny, as recorded in single zircon crystals (Rhodope zone, Greece). *Gondwana Research* **29**, 199–207.

Lilov P, Maliakov Y and Balogh K (2004) K-Ar dating of metamorphic rocks from Strandja massif, SE Bulgaria. *Geochemistry, Mineralogy and Petrology (Sofia)* **41**, 107–20.

Machev PH, Ganev V and Klain L (2015) New LA-ICP-MS U-Pb zircon dating for Strandja granitoids (SE Bulgaria): evidence for two-stage late Variscan magmatism in the internal Balkanides. *Turkish Journal of Earth Sciences* **24**, 230–48.

Malyakov Y and Bakalova DG (1978) The Lower Permian near the village of Kondolovo Strandja Mountain. *Comptes Rendus de l'Academie bulgare des Sciences* **31**, 715–8.

Malyakov Y and Prokop RP (1997) Prevue paleontologiques (Crinoides devoniennes) pour l'age de certaines roches epimetamorphiques du Strandja bulgare. *Comptes Rendus de l'Academie bulgare des Sciences* **50**, 99–102.

McDougall I and Harrison TM (1999) *Geochronology and Thermochronology by the $^{40}Ar/^{39}Ar$ Method*, Second Edition. Oxford University Press, Oxford, 269 pp.

Natal'in B, Sunal G, Gun E, Wang B and Zhiking Y (2016) Precambrian to Early Cretaceous rocks of the Strandja Massif (northwestern Turkey): evolution of long-lasting magmatic arc. *Canadian Journal of Earth Sciences* **53**, 1312–35.

Natal'in B, Sunal G, Satir M and Toraman E (2012) Tectonics of the Strandja Massif, NW Turkey: history of long-lived arc at the northern margin of Palaeo-Tethys. *Turkish Journal of Earth Sciences* **21**, 755–98.

Neubauer F, Bilyarski S, Genser J, Ivanov Z, Peytcheva I and von Quadt A (2010) Jurassic and Cretaceous tectonic evolution of the Sakar and Srednogorie zones, Bulgaria: ^{40}Ar/^{39}Ar mineral ages and structures. In *Proceedings of the XIX Congress of the Carpathian-Balkan Geological Association*, Thessaloniki, Greece, 23–26 September 2010. *Geologica Balcanica* 39, 1–2, 273–4.

Okay AI, Satır M, Tüysüz O, Akyüz S and Chen F (2001) The tectonics of Strandja Massif: late-Variscan and mid-Mesozoic deformation and metamorphism in the northern Aegean. *International Journal of Earth Sciences* **90**, 217–233.

Palshin IG, Skenderov GM, Bozkov B, Mihailov JN, Kotov EI, Bedrinov IT and Ivanov IM (1989) New geochronological data on the Cimmerian and Alpine magmatic and hydrothermal formations in Srednogorie and Stara Planina zones, Bulgaria. *Review of the Bulgarian Geological Society* **40**, 75–91.

Pamir HN and Baykal F (1947) The geological structure of the Strandja Massif. *Bulletin of the Geological Society of Turkey* **1**, 7–43.

Savov S and Dabovski Ch (1980) The metamorphic Triassic in Topolovgrad syncline. In *The Precambrian in south Bulgaria* (eds Kozhoukharov D and Dabovski C), pp. 127–32. Bulgaria, October 1980, Bulgarian Academy of Sciences, Geological Institute, Guide to Excursion IGCP project 22.

Sunal G, Natal'in B, Satir M and Toraman E (2006) Paleozoic magmatic events in the Strandja Massif, NW Turkey. *Geodinamica Acta* **19**, 283–300.

Sunal G, Satir M, Natal'in BA, Topuz G and Vonderschmidt O (2011) Metamorphism and diachronous cooling in a contractional orogen: the Strandja massif, NW Turkey. *Geological Magazine* **148**, 580–96.

Sunal G, Satir M, Natal'in B and Toraman E (2008) Paleotectonic position of the Strandja massif and surrounding continental blocks based on zircon Pb-Pb age studies. *International Geology Review* **50**, 519–45.

Szopa K, Salacinska A, Gumsley AP, Shew D, Petrov P, Gaweda A, Zagorska A, Deput E, Gospodinov N and Banasik K (2020) Two-stage Late Jurassic to Early Cretaceous hydrothermal activity in the Sakar unit, Southeastern Bulgaria. *Minerals* **10**, 16 pp.

Villagómez D and Spikings R (2013) Thermochronology and tectonics of the Central and Western Cordilleras of Colombia: Early Cretaceous-Tertiary evolution of the Northern Andes. *Lithos* **160–161**, 228–49.

Zacharieva-Kovacheva K, Ware S and Chatalov G (1964) Geological age of low metamorphic rocks north of Golyam Dervent, SE Bulgaria. *Comptes Rendus de l'Academie bulgare des Sciences* **17**, 749–51.

https://doi.org/10.1017/S0016756820000953 Published online by Cambridge University Press